

CR-1777-209234

11/11/99

**Yearly Progress Report
NRA-97-MTPE-04**

**“HALOE Algorithm Improvements for
Upper Tropospheric Sounding”**

March 11, 1999

**Martin J. McHugh
Larry L. Gordley**

**GATS, Inc
11864 Canon Blvd., Suite 101
Newport News, VA 23606**

**James M. Russell III
Center for Atmospheric Sciences
Hampton University
Hampton, VA 23668**

**Mark E. Hervig
Dept. of Atmospheric Science
University of Wyoming
Laramie, WY 82071**

HALOE Algorithm Improvements for Upper Tropospheric Sounding

TABLE OF CONTENTS

EXECUTIVE SUMMARY	3
BACKGROUND	4
OVERVIEW OF TASKS	5
ACCOMPLISHMENTS.....	5
1. POINTER-TRACKER	5
<i>Gimbal angle analysis</i>	5
<i>Refraction correction</i>	6
2. CLOUD/AEROSOL IDENTIFICATION AND CHARACTERIZATION.....	7
<i>Background</i>	7
<i>Tropopause proximity</i>	7
<i>Magnitude-based discrimination</i>	8
<i>Gradient-based discrimination</i>	8
<i>Spectral discrimination</i>	8
<i>Results</i>	9
<i>Summary</i>	11
3. MULTICHANNEL RETRIEVAL	11
<i>Background</i>	11
<i>"Differential retrieval" of water vapor</i>	11
<i>Application to cloud contaminated data</i>	13
<i>Summary</i>	13
4. FORWARD MODEL IMPROVEMENTS.....	13
<i>Background</i>	13
<i>Methane line mixing</i>	14
5. FINE VERTICAL RESOLUTION GAS CHANNEL RETRIEVALS	14
6. IMPROVED TEMPERATURE-PRESSURE RETRIEVAL.....	14
7. ERROR ESTIMATES	15
8. LONG TERM TREND ANALYSES	15
<i>Background</i>	15
<i>Gas-cell content</i>	15
<i>Pointing accuracy</i>	15
<i>Summary</i>	16
9. DATA VALIDATION.....	16
<i>Correlative studies</i>	16
<i>V19 validation</i>	16
SCHEDULE/PLANS	16
BIBLIOGRAPHY.....	18

HALOE Algorithm Improvements for Upper Tropospheric Sounding

Executive Summary

This Mission to Planet Earth Initiative is part of the UARS Science Investigator Program. The objective of this research is to improve and augment the processing algorithms for the Halogen Occultation Experiment (HALOE). HALOE has been operating since 1991, measuring O₃, H₂O, HCl, HF, NO₂, NO and CH₄, temperature/pressure and aerosol extinction at four wavelengths. Primary goals of this project include: extending the water vapor, ozone and methane retrievals into the upper and middle troposphere; providing a cloud height data set; increasing the accuracy of the retrievals in the stratosphere; and improving the vertical resolution of the gas-cell species.

At the end of the first year of this proposed three-year research effort, we are ahead of the initial schedule in several areas. Two main accomplishments are a cloud-top data set and a differential water vapor retrieval. The cloud-top detection algorithm identifies clouds in the measurements by examining the spectral profile of the aerosol extinction. A HALOE cloud-top pressure/altitude data set has been created with this technique, and a complete description has been accepted for publication in GRL. In the initial effort to improve the water vapor retrieval in conditions of high particulate loading, a differential retrieval technique was tested and implemented. This is a special case of a general multichannel retrieval, simultaneously using signals from the 6.61 and 6.25 μm channels to reliably retrieve water vapor with little sensitivity to aerosol or cloud contamination. The differential retrieval has been used successfully to correct a set of zonal mean water vapor results that were corrupted by polar mesospheric clouds. We are now able to use the technique to verify and improve our aerosol correction in the water channel.

The cloud-top data and the differential algorithm are important improvements to the HALOE data product, and are essential in the progress towards improved tropospheric sounding. Additional accomplishments from the first year include an improved tropopause location method, analysis of the pointer/tracker algorithm, instrument trend reliability assessment and progress on the general multichannel retrieval. Remaining proposed tasks include completion of the multichannel inversion algorithm development, improvements to the forward models, more accurate cloud/aerosol characterization, extending the limits of the pressure-temperature retrieval, and improving the vertical resolution of the gas-cell species. This work will significantly enhance the utility of the already valuable HALOE measurements, extending this unique and important data set for atmospheric research.

Background

The HALOE instrument aboard the UARS platform provides solar occultation measurements of seven trace gases, temperature/pressure and aerosol extinction at four wavelengths (see Table 1, and e.g. Russell et al.¹). Additional derived products include aerosol size distribution, surface area density, and composition. HALOE has remained fully operational since it was activated October 11, 1991, with no appreciable degradation in performance characteristics to date.

Table 1 — Species, wavelength and typical altitude ranges for Version 19 HALOE data

Species	Wavelength (μm)	Altitude Range (km)
O_3	9.85	10 – 90
H_2O	6.60	10 – 85
NO_2	6.25	15 – 50
NO	5.26	15 – 140
CH_4	3.46	15 – 75
HCl	3.40	15 – 60
T/P	2.80	35 – 90
HF	2.45	15 – 60
Aerosol	5.26 3.46	10 – 50
	3.40 2.45	

HALOE data are used by researchers worldwide. The utility of the data is exemplified by the volume of requests from the DAAC* and the HALOE web site[†]: in FY97 there were over 25 Gigabytes served filling over 110,000 requests for HALOE data (excluding internal use). The HALOE web site usage is shown in Fig. 1. This web site was implemented to aid the post-launch validation effort, efficiently serving the HALOE science team and associates. It was continued in that capacity, and upon initial release of the HALOE data, the web site was opened to the public.

Motivation for this work stems from the intense interest by the research community in the upper troposphere. For example: upper tropospheric water vapor and ozone are crucial

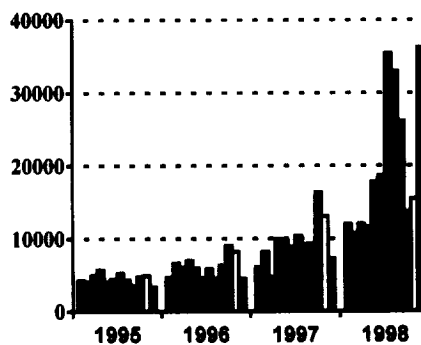


Fig. 1 — HALOE web site queries by month from 1995 through 1998. A query is defined as downloading any NetCDF or SPF file, or viewing a GIF image

elements in questions involving radiative forcing; cloud formation affects the heat budget and heterogeneous chemistry; methane is a major “greenhouse” gas. The importance of these constituents in the upper troposphere warrants the effort needed to push the HALOE data set to the lowest possible altitudes.

While current Version 19 (V19) processing produces data well beyond original HALOE objectives, there is still a wealth of untapped information at the lowest altitudes. For example, water vapor is currently retrieved from the 6.60 μm (H_2O) channel, and while this provides excellent signal to noise ratios throughout the

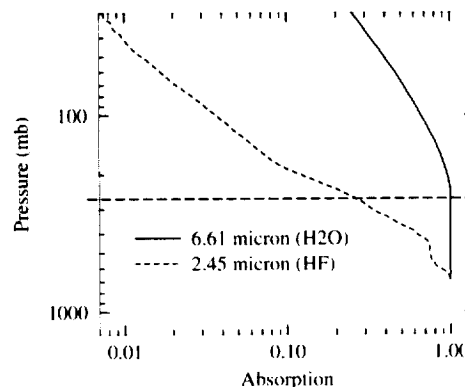


Fig. 2 — Absorption profiles from the 6.61 and 2.45 μm channels for a HALOE sounding (25-Aug-1996 sunset near 73°N 294°E). V19 uses the 6.61 μm channel to retrieve water vapor. In this example, the 6.61 μm channel saturates near the tropopause (horizontal line). The 2.45 μm channel, consisting primarily of weak water absorption below the tropopause, remains viable to 600 mb.

* Distributed Active Archive Center at Goddard Space Flight Center: <http://daac.gsfc.nasa.gov>

† <http://haloedata.larc.nasa.gov>

stratosphere, the signals rapidly become saturated in the troposphere. We can shift to the 2.45 μm (HF gas correlation) channel at these lower altitudes, where water vapor is the dominant absorber but the signal does not saturate as quickly (see Fig. 2). This principle is most fully exploited in the form of a multichannel or vector retrieval, combining information from multiple channels in an optimal fashion. Using this technique, coupled with improved forward models and aerosol/cloud characterization, we can expect to retrieve ozone, water vapor and methane into the middle troposphere, and NO and HCl into the upper troposphere.

Overview of Tasks

This project consists of nine major objectives, primarily aimed at extending the HALOE retrievals into the troposphere. These tasks are highly coupled, in some instances requiring several iterations to achieve the best possible results, with several tasks spanning all three years of the project's proposed term. A complete description is found in the original proposal, and they are summarized here.

1. **Advanced Pointer Tracker Analysis:** Attempt to use gimbal angle information to compliment ephemeris data and refraction model, increasing the pointing accuracy in cases of severe attenuation.
2. **Cloud/Aerosol Identification and Characterization:** Develop a cloud detection algorithm using the spectral extinction measurements, and create a cloud-top height data set. Improve tropospheric aerosol modeling in the radiometer (O_3 , H_2O , NO_2 and CO_2) channels.
3. **Simultaneous Multichannel Inversion Algorithm:** Develop and implement multichannel retrievals that will optimally combine information from several wavebands to extract the maximum tropospheric signal information. This will push the lower bounds of the retrievals beyond the limits encountered by the current algorithm.
4. **Forward Model Improvements:** Increase the accuracy of forward models where possible, especially the O_3 and CO_2 models.
5. **Fine Vertical Resolution Gas-cell Retrievals:** Develop efficient code to enable processing at higher vertical resolution of the

gas-cell species (NO , CH_4 , HCl and HF), making them commensurate with the radiometer channels and instrument resolution.

6. **Improved Pressure-Temperature Retrieval:** Exploit CO_2 and aerosol forward model improvements to extend the lower limit of the retrieved pressure, relaxing the dependence on auxiliary NCEP* temperature data.
7. **Robust Error Estimates:** Produce estimates of the random and systematic variance of the data, which will be included with current precision estimates.
8. **Long-term Trend Reliability Studies:** Develop procedures to routinely monitor and quantify the stability of the instrument, particularly the gas-cell content, pointing performance, optical and spectral responses.
9. **Data Validation:** Coordinate studies with the HALOE science team and correlative measurement providers to validate and document results.

Accomplishments

The first year of this project yielded two major accomplishments: a cloud identification algorithm resulting in the cloud height dataset, a cloud correction procedure, and a differential retrieval technique for water vapor. Other important contributions were made in the areas of pointing/tracking, forward model improvements and trend analysis. In this section, we present the first year's results in detail, as we review the progress made on each task and the obstacles remaining.

1. Pointer-tracker

Gimbal angle analysis

The HALOE instrument tracks the top of the sun with a visible (0.7 μm) fine sun sensor, and the telescope is "locked-down" at a fixed angle, typically 8 arcmin, below the sun sensor. The angular resolution of the detectors in the fine sun sensor is 16 arcsec, and the resulting accuracy of the pointing system is approximately 8 arcsec, translating to about 100 m at the tangent point. Accurate pointing information is critical to model the solar source function correctly and to register the data to tangent point altitudes.

* National Center for Environmental Prediction, formerly National Meteorological Center

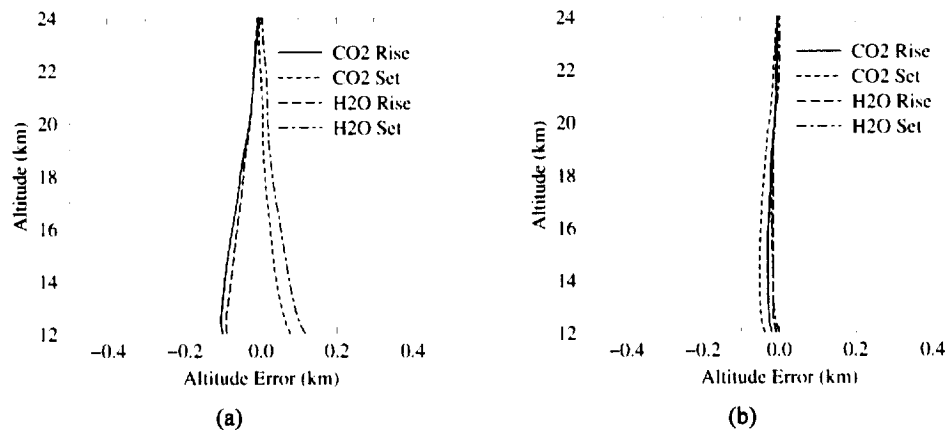


Fig. 3 — Apparent altitude errors in the H₂O and CO₂ channels, derived from rise-set crossover measurements taken with lockdown angles of 8 and 12 arcmin during Jan.-Feb. 1997 near 70°S. a) Errors derived from Version 18 data, which used the mean tracker output. b) Errors derived from V19 data, which uses the instantaneous tracker signal. These are now within the accuracy that can be achieved with a gimbal angle analysis.

In cases of high attenuation, there were indications that the tracking system was biased. These suspicions arose after close examination of “crossover” data, where the orbital geometry yields both sunrise and sunset occultations at nearly identical latitudes. In such cases, the atmospheric variability between events should be small (for non-diurnal gases), so any consistent difference between the rise and set modes indicates a measurement bias. Such a bias was noticed in HALOE water vapor data, and careful consideration led to the hypothesis that the tracker was wandering when the sun was heavily attenuated by the lower stratosphere and upper troposphere. Efforts then began to improve our pointing angle knowledge by exploiting gimbal angle information. However, we would discover that the tracking problems all but vanish in the V19 data set.

The studies that motivated this work were carried out on Version 18 data (V19 began processing in May 1998). In V18 processing, the pointing angle relative to the top edge of the sun was estimated by the mean of the tracker output, and this constant angle was used for all altitudes. In V19, the pointing angle is estimated at each individual altitude by the instantaneous tracker output.

We analyzed data collected in cases where the HALOE instrument had been commanded to alternate lockdown positions between 8 and 12 arcmin every other orbit. We derived the altitude shift of mean transmission signals between similar measurements taken at the different lockdowns. The altitude shift was then mapped as a function of the top solar edge altitude.

Example results are shown in Fig. 3. Using this diagnostic, it became apparent that using the mean lockdown (V18) rather than instantaneous lockdown position (V19) was the major cause of sunrise-sunset differences in the lower stratosphere, *not* tracker error. Differences vanished in V19 except for very infrequent situations when the beta angle* exceeds 60°. Evidence now suggests that these rare differences may be the result of thermally induced motion between the tracker and the telescope.

Hence, the tracker signals as used in V19 are believed to be accurate and would not be improved by information from onboard gimbal angle signals. Still, there is potential to employ gimbal angle information as a diagnostic, warning of extreme tracker error as occurs in heavy attenuation.

Refraction correction

Another pointing issue that has been identified involves the refraction calculation. V19 processing calculates refraction for the 2.80 μm band, and no corrections are made for other channels. This has negligible effect above 150 mb and was sufficient for the altitude ranges in the current data. As we push into the troposphere, however, the refraction differences between wavebands become appreciable, so we will need to use a wavelength specific refraction model. A plan for implementing this correction has been devised.

* Beta angle refers to the angle between the orbital plane and the earth-sun direction

2. Cloud/Aerosol Identification and Characterization

Background

There is considerable interest in cirrus clouds because of their role in radiative forcing² and heterogeneous ozone chemistry³. They are also one of the most important considerations in remote sounding below the tropopause: they can dominate extinction and are spectrally distinct from sulfate aerosols, therefore must be identified and treated differently. Identification of clouds in the HALOE data is therefore a high priority, and a necessity for successful tropospheric retrievals.

Cirrus clouds are difficult to model in a limb viewing geometry because of their local field of view and episodic nature. Kent et al. have studied these problems as related to SAGE II.⁴ Attempts to use thermodynamic criteria to identify clouds in HALOE data have been largely unsuccessful because of these properties, compounded by inadequate accuracy in tropospheric temperature and water vapor content. To overcome this, we have developed a method that reliably detects clouds in the HALOE measurements, based on the extinction spectra. Because of the significance of this result, a summary of the work has been published in Geophysical Research Letters.⁵ Here we present a description of our efforts and summarize the pertinent results.

Tropopause proximity

Cirrus form in the vicinity of the tropopause because of the cold temperatures and enhanced water vapor content. Consequently, knowing the tropopause height can guide the search for cirrus clouds. In this work, we will search for clouds

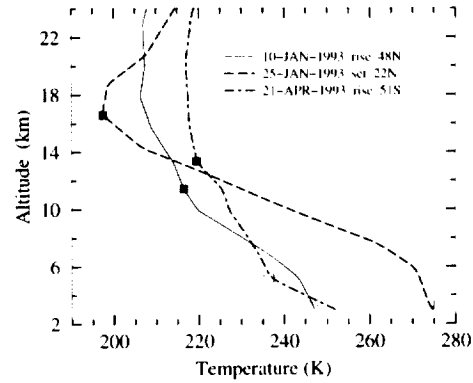


Fig. 4 — Examples of erroneous V19 HALOE tropopause locations. Open boxes are V19 tropopause heights and filled boxes show the heights found with new 2-point technique. These examples are extremely rare, but accurate tropopause location is critical for cirrus identification. (Note: HALOE temperatures below 30 km are from the NCEP analysis.)

no higher than 4 km above the tropopause.

Current (V19) HALOE data contain tropopause heights, but because of its importance here, we reviewed the algorithm used to determine these and found that some modification was necessary. The V19 algorithm identifies the tropopause as the lowest point where the estimated lapse rate ($-dT/dz$) is less than 2 K/km. The lapse rate is estimated by the least mean-square slope of the temperatures over eight 0.3 km layers and assigned to the lowest of the eight layers. Careful examination reveals occasional instances where this gives incorrect results. A slightly more robust definition was constructed by simply estimating the lapse rate from the temperature difference between

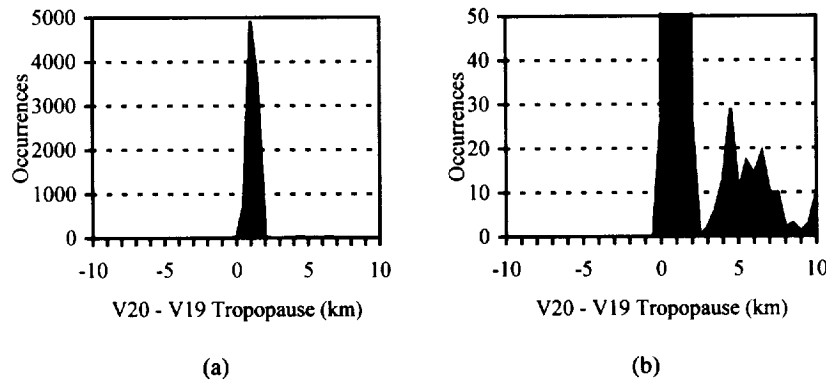


Fig. 5 — Version 20 minus V19 tropopause height differences for all 1993 HALOE data (9356 profiles). a) The average difference is about 1 km, with V19 lower than Version 20. b) On a magnified scale, cases with large differences can be resolved.

adjacent layers. The tropopause is again declared when the lapse rate falls below 2 K/km, with the proviso that it remains so for at least 2 km above. This should more closely mirror the concept of thermodynamic tropopause location in a continuous temperature profile.

Fig. 4 shows examples where the V19 algorithm gives incorrect results which the modified definition remedy. Apparent in these examples is the inherent vertical resolution of approximately 2 km in the temperature data, which are derived from the NCEP database at these altitudes. Because of this, averaging eight layers is unnecessary, and in fact, causes the errors witnessed in Fig. 4. Results from the new two-point tropopause algorithm and V19 for all 1993 HALOE profiles are compared in Fig. 5. Heights from V19 are typically about 1 km lower than from the new algorithm and occasionally more than 5 km too low. These differences are large enough to be significant in cloud identification, so the new two-point tropopause algorithm was adopted for this work and will be incorporated into V20.

Magnitude-based discrimination

Extinctions in clouds are typically much larger than from aerosol, mainly because cloud particle sizes are larger. The extinction magnitude discriminant has been used in SAGE* measurements analyses.⁶ However, in the heavy volcanic conditions following the eruption of Mt. Pinatubo, aerosol and cloud extinction magnitudes overlap and clouds cannot be recognized based on magnitude without additional constraints.

Gradient-based discrimination

Clouds are also characterized by their rather well defined (compared to the ~2 km HALOE resolution) upper boundary. A HALOE extinction profile containing clouds will have a rapid increase in extinction descending into the cloud-top, in contrast to sulfate aerosol layers. An obvious example is shown in Fig. 6. The vertical gradient of the extinction can therefore be a useful criterion to differentiate cloud from aerosol. We define the gradient as

$$G = -\frac{\log_{10} \beta_i(z_2) - \log_{10} \beta_i(z_1)}{z_2 - z_1}, \quad (1)$$

where z_1 and z_2 are the altitudes of adjacent layers and β_i is the extinction coefficient for waveband i . In the stratosphere, the HALOE

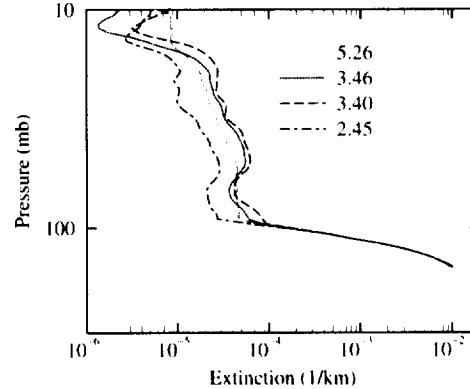


Fig. 6 — HALOE extinction profiles from 5-Jan-1997 sunset at 15°N 330°E. The horizontal line indicates the tropopause. The sudden large vertical gradient and the accompanying spectral uniformity of the extinctions indicate clouds.

5.26 μm channel provides the most reliable extinction measurements, and we use this channel whenever extinction estimates for a single waveband are required.

Unfortunately, contaminant absorption in the troposphere, primarily from water vapor and methane, corrupts the lower portion of the extinction profiles. The typical result of this is artificially high gradients moving into the troposphere, which can be mistaken for clouds.

A further difficulty with this approach is determining the appropriate threshold level for G . A realistic model of the measured gradients would be quite complex, and no obvious way to validate the model is apparent. However, a straightforward statistical analysis of the metric can be done if we identify a subset of the data that we know to contain clouds. In the next section we present a method that enables us to do just this.

Spectral discrimination

Another observed distinction between clouds and aerosol is the spectral dependence of the extinctions (Fig. 6). Again because the particles are relatively large (>10 μm effective radius), clouds cause nearly uniform extinction over the wavelengths measured by HALOE. Sulfate aerosol extinction on the other hand exhibits a distinct wavelength dependence, the exact form of which depends on the specific particle-size distribution.

A direct measure of spectral uniformity, utilizing all four extinctions, is the variance

$$\sigma^2 = \left(\frac{1}{4} \sum_{i=1}^4 \beta_i^2 \right) - \mu^2, \quad (2)$$

* Stratospheric Aerosol and Gas Experiment

where β_i are the four HALOE extinction coefficients and μ is their mean. However, the variance is sensitive to the magnitude of the extinctions, and using it as a discriminant for clouds—selecting all cases with variance below some threshold—would preferentially select cases where the extinctions are small. HALOE extinctions typically span many orders of magnitude, so this is an unsuitable choice as a discriminant. To avoid this problem, we normalize the variance by the square of the mean

$$\hat{\sigma}^2 = \frac{\sigma^2}{\mu^2} \quad (3)$$

forming a measure that is insensitive to the scale of the extinction. A geometrical approach to the problem provides some insight and justification for this metric. If we construct the four-dimensional vector $\beta = (\beta_1, \beta_2, \beta_3, \beta_4)$ we can compute the angle, θ , between β and a vector in the “white” direction, $\mathbf{n} = (1, 1, 1, 1)$:

$$\cos \theta = \frac{\beta \cdot \mathbf{n}}{|\beta| |\mathbf{n}|} \quad (4)$$

When $\cos \theta$ is near unity, the extinctions are white—indicative of clouds. A bit of manipulation reveals that

$$\hat{\sigma}^2 = \tan^2 \theta, \quad (5)$$

so the normalized variance is an equivalent measure of spectral whiteness.

Because the spectral shape of the extinction is preserved through the various measurement and modeling errors involved in deriving the extinction coefficients, we can be reasonably certain that the normalized variance given by (2) and (3) will be a faithful cloud detector when a sufficiently tight threshold is set. Unlike the gradient metric, we can determine a threshold rather simply from *a priori* system characteristics. Ideally, the metric approaches zero when dominated by cloud extinction. A simple analysis shows that when corrupted by noise, the metric increases from the true value by a bias:

$$\langle \hat{\sigma}^2 \rangle \approx \hat{\sigma}^2 + \langle \delta^2 \rangle / \mu^2 \quad (6)$$

Here $\langle \rangle$ represents expected value, $\hat{\sigma}_0^2$ is the noiseless value and $\langle \delta^2 \rangle$ is the variance of the additive, zero-mean independent noise. Typical HALOE extinction uncertainties (δ/μ) are less than 10% as inferred from correlative O_3 and

H_2O measurements, so we are unlikely to have false detections if we declare clouds whenever $\hat{\sigma} < 0.10$. Statistical examination of the metric using the complete set of HALOE profiles indicates that raising this threshold to 0.15 is a reasonably conservative choice. To further validate this method, comparisons were made with NOAA AVHRR* imagery. These qualitative results were also favorable: clouds appeared in the AVHRR images where the spectral metric predicted and were absent in the others.

Results

The methods described above (extinction magnitude, vertical gradient, and spectral uniformity) were applied to HALOE measurements and assessed, to arrive at a suitable configuration of tests for cloud-tops. After screening a large number of HALOE profiles with the spectral metric, it appears that while the metric has nearly perfect probability of detection, a small number of profiles with obvious cloud contamination are missed. On these occasions, clouds are evident by every other measure, but the spectral metric *increases* rather than approach zero. In such cases it is invariably found that one of the retrievals, usually water or methane, halted higher than usual and climatology was substituted. This in turn caused the aerosol retrievals to be unreliable. While the proposed multichannel water and methane retrievals will alleviate this to a great extent, an immediate solution is needed.

In order to set the threshold for the gradient metric, G , we now use the spectral metric to assemble a collection of known cloud-contaminated profiles. By choosing the highly conservative criterion of $\hat{\sigma} < 0.05$ the resulting profiles are almost certainly contaminated with clouds. Examining the distribution of gradient metric values from these data indicates that choosing a limit of 0.3 km^{-1} is nearly optimal for these heavy cloud conditions. For more tenuous clouds, the signature will be a linear combination of cloud and sulfate extinctions. Efforts to separate the relative contributions of each constituent are being investigated.

Finally, to prevent erroneous identification from an anomalous single layer, we require that the metrics exceed their thresholds in three or more consecutive 0.3 km layers. This is nearer

* National Oceanic and Atmospheric Administration's Advanced Very High Resolution Radiometer

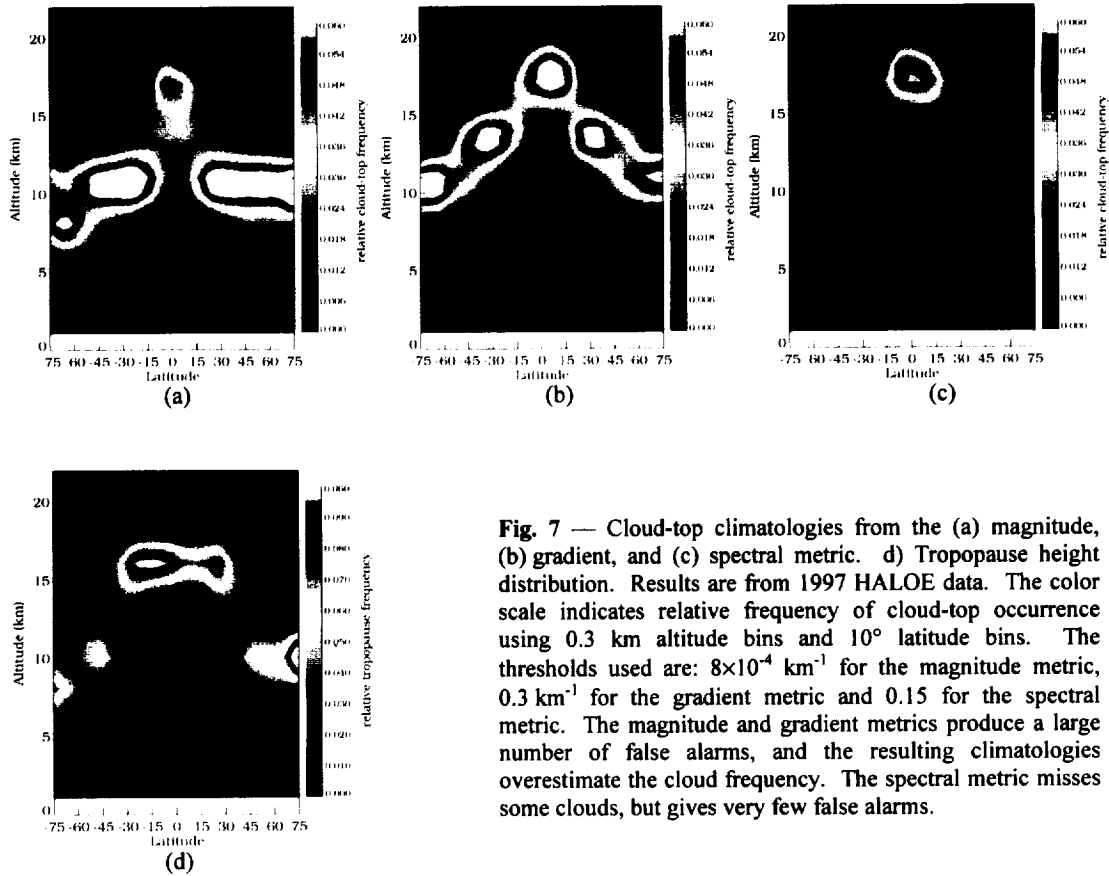


Fig. 7 — Cloud-top climatologies from the (a) magnitude, (b) gradient, and (c) spectral metric. (d) Tropopause height distribution. Results are from 1997 HALOE data. The color scale indicates relative frequency of cloud-top occurrence using 0.3 km altitude bins and 10° latitude bins. The thresholds used are: $8 \times 10^{-4} \text{ km}^{-1}$ for the magnitude metric, 0.3 km^{-1} for the gradient metric and 0.15 for the spectral metric. The magnitude and gradient metrics produce a large number of false alarms, and the resulting climatologies overestimate the cloud frequency. The spectral metric misses some clouds, but gives very few false alarms.

the instrument's vertical resolution without being overly restrictive.

Cloud climatologies generated with the individual metrics from 1997 HALOE data are shown in Fig. 7. With a threshold at $8 \times 10^{-4} \text{ km}^{-1}$, the magnitude metric generates a significant number of false alarms. Unfortunately, raising this threshold causes an unacceptable number of missed detections. Because of this and for reasons given above, the magnitude metric is not considered a reliable indicator.

As expected, contaminant water and methane absorption cause false alarms from the gradient metric, while the spectral metric suffers missed detections. This contrasting behavior yields vastly differing total probabilities of cloud occurrence, shown in Fig. 8. From this it is apparent that the gradient metric greatly overestimates the number of cloud contaminated profiles. We therefore choose to rely instead on the spectral metric as our final cloud identifier, with the caution that some cloud-contaminated profiles will be missed.

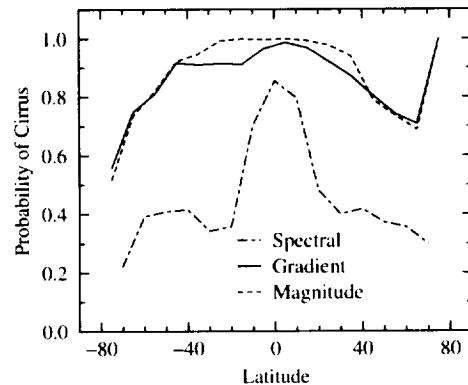


Fig. 8 — Probability of clouds as predicted by each metric using 1997 HALOE data. These are the cumulative statistics from Fig. 7. False alarms plague both the magnitude and gradient metrics. The spectral metric misses some detections, but generally produces reasonable cloud frequency statistics.

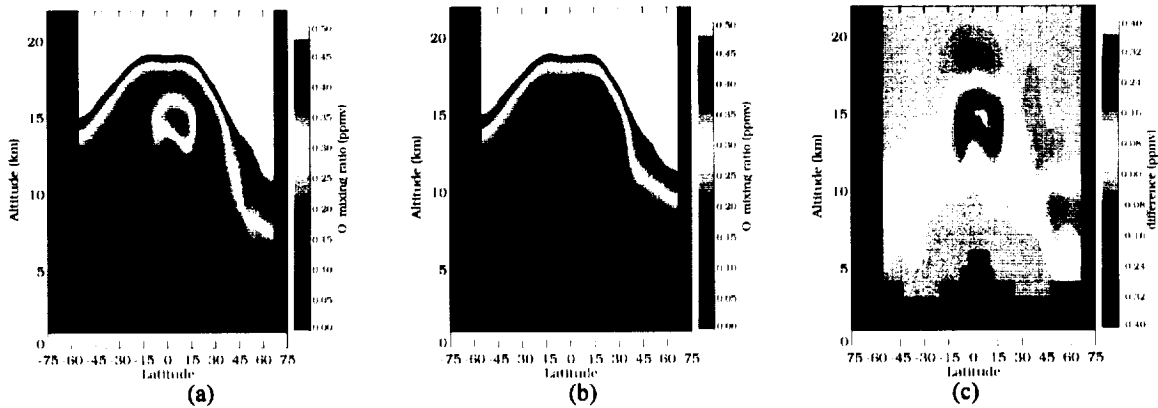


Fig. 9 — Effect of cirrus filtering on HALOE ozone data. a) Latitude vs altitude cross-section of V19 HALOE ozone for sunrises from March 22 to April 19, 1995 (368 profiles). Only altitudes below 22 km are shown. Color indicates mixing ratio on a magnified scale (0–0.5 ppmv) to resolve the relatively small tropospheric values (stratospheric values exceed 10 ppmv). b) The same data after cirrus filtering using the spectral metric. Profiles now extend only down to identified cloud-tops. c) The difference: V19 minus filtered. An artifactual “bubble” of tropical ozone that is removed by cirrus filtering is evident.

After cloud-top heights have been identified, we can excise the contaminated portions of the retrievals, forming a cloud-free data set. The effect of cloud screening on HALOE ozone is shown in Fig. 9. A similar screening has recently been used by Bhatt, et al.⁷, using a gradient-based approach. Notice that the unrealistically high ozone concentration near the tropical tropopause in the V19 data is removed by the cloud filtering, indicating that it was artifact induced by cloud contamination.

It is conceivable that one could retrieve through thin clouds by correctly modeling and extrapolating the extinction to the CO₂, water and ozone radiometer wavelengths. However, because of the sporadic and localized nature of the clouds, this is fraught with uncertainty, and has not yet been attempted.

Summary

In summary, a robust algorithm for identifying clouds in HALOE data has been constructed and tested. The algorithm declares clouds whenever $\hat{\sigma} < 0.15$ for three consecutive 0.3 km layers, searching up to 4 km above the tropopause. Tropopause heights were determined from a new V20 technique. Cloud-top heights for the entire database have been assembled and will be available on the HALOE web page*. HALOE data can now be screened for cloud contamination, and cloud-filtered ozone data have been presented. This represents

a new and important data product for the HALOE program, and a necessary tool for improved upper tropospheric sounding.

3. Multichannel Retrieval

Background

The HALOE filter bandpasses were chosen specifically for retrieving specific gases in the stratosphere. While these results have been excellent, we seek to extend the altitude range of the retrievals now by combining information from multiple wavebands (e.g. Fig. 2). The most general form of this is a multi-channel, multi-gas vector inversion where multiple species are retrieved from the entire set of measurements simultaneously. Current processing uses an onion peel method, retrieving single species in an iterative fashion. While the complete generalized form has theoretical appeal, in practice there are enough limitations that a specialized version of the multichannel retrieval becomes the most useful choice.

“Differential retrieval” of water vapor

Our first step toward developing a multichannel inversion is a dual-channel differential water vapor retrieval. This simple yet powerful method exploits the spectral proximity of the 6.61 μm (H₂O) and 6.26 μm (NO₂) radiometer channels. Because they measure at nearly the same wavelengths, they can be used simultaneously to retrieve water vapor without any *a priori* aerosol extinction information. This is extremely useful when

* <http://haloedata.larc.nasa.gov>

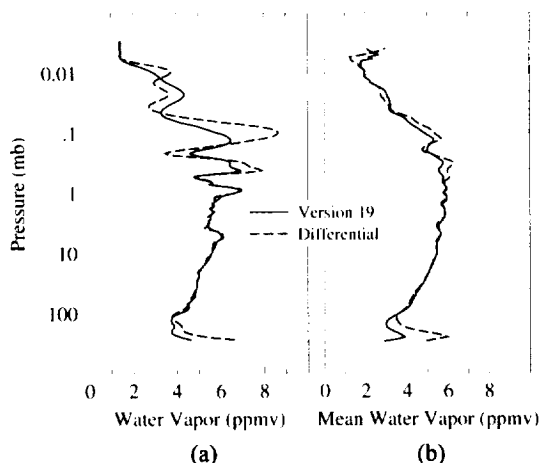


Fig. 10 — Differential water retrieval compared to V19 for HALOE Sunset 29-Mar-1995 near 52°N. a) Retrievals for a single occultation (114°E). Differences near the tropopause (horizontal line) are indicative of cirrus contamination corrupting V19. The typically large variations in the mesosphere are amplified in the differential retrieval from the 6.26 μm channel noise. b) Daily mean of the V19 and differential method. Averaging reduces the variability in the mesosphere.

clouds are present in the line of sight making the aerosol measurements unreliable.

The V19 water vapor retrieval uses the 6.61 μm channel. The aerosol absorption in this waveband is extrapolated from the extinction retrieved in the 5.26 μm gas correlation channel, assuming a sulfate aerosol model. When sensing through clouds, errors are introduced as the sulfate model becomes unrealistic. However, because aerosol extinction is a slowly varying function of wavelength, it should contribute nearly equally to the 6.61 and 6.26 μm channels. Our differential method retrieves water vapor by modeling the *differential ratio*

$$\rho \equiv 1 - \tau_{6.6} / \tau_{6.26} \quad (7)$$

where τ_λ is the transmission in waveband λ . This quantity is nearly independent of aerosol absorption. Interfering absorbers (O_3 , CH_4 and NO_2 in these wavebands) are inferred from previous retrievals and/or climatology as appropriate.

Fig. 10a compares the differential water retrieval to V19 for an individual occultation. Below 100 mb, differences arise from cloud contamination in the V19 retrieval. No aerosol model is used in the differential retrieval. While the differential method improves the results in

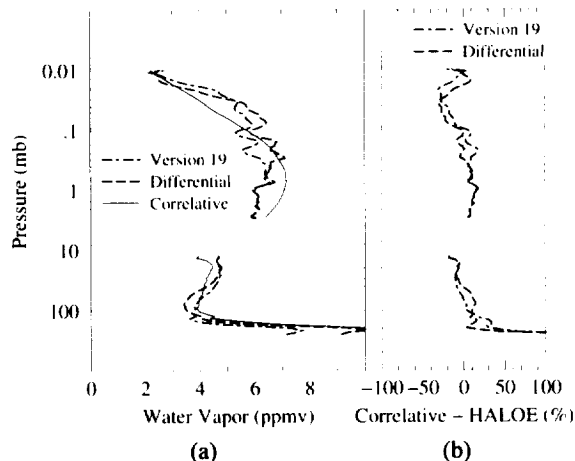


Fig. 11 — Comparison of HALOE water vapor from the differential retrieval and V19 to correlative measurements. a) Mean profiles for differential, V19, and correlative. b) Mean differences between the correlative measurements and HALOE, for the differential retrievals and V19. Notice the differential is in closer agreement between ~100 to 200 mb. *Upper* — Bevilacqua ground based mm-wave: 12 profiles near 45°S, 15-Sep-1994. *Lower* — Oltmans balloon frost point hygrometer: 15 profiles near 40°N, 19-Mar-1993.

clouds, the saturation of the signal in the 6.61 μm band still plagues the retrieval, and the results become unreliable nearing the tropopause. This problem will be dealt with most effectively by the multichannel retrieval now in progress, in which we shift emphasis to the 2.45 μm channel below the tropopause to overcome the signal saturation here.

In the mesosphere (above 1 mb in Fig. 10), the differential retrieval exhibits large variability. This is because the 6.26 μm channel is relatively noisy in this region, amplifying the already large uncertainty here. Fortunately, this variability is less problematic in the daily (zonal) mean, as illustrated by Fig. 10b. As a time saving device, daily mean profiles are retrieved directly from the daily mean transmission signals, rather than by averaging the individually retrieved profiles. Case studies have validated that retrievals from the mean signals are equivalent to the daily means of retrievals to within the measurement precision.

Fig. 11 shows a comparison of the differential retrieval and V19 to correlative water vapor measurements. Overall, the differential method agrees roughly as well as V19, but note that while V19 differences become large below 100 mb, the differential results agree well until about 200 mb. The deterioration below this is,

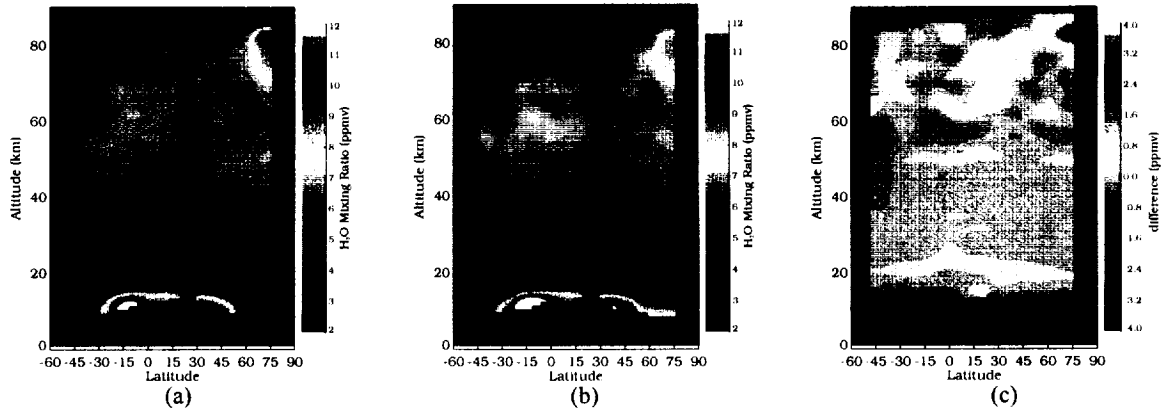


Fig. 12 — HALOE water vapor for a latitude sweep of sunrise occultations from 29-Jun to 13-Aug 1995. a) V19 results show extremely high concentrations (>11 ppmv) in the mesosphere at high northern latitudes. b) Differential retrieval results. The maximum mesospheric water concentrations are now abated, reaching only ~9 ppmv. c) Differential – V19 differences. The red spot suggests PMCs corrupted the V19 retrievals but not the differential. The blue region indicates light cirrus conditions where the V19 aerosol model loses accuracy. All retrievals here were carried out on the daily mean signals.

as noted above, from the saturation of the 6.61 μm channel.

Application to cloud contaminated data

Being insensitive to particulate absorption, the differential retrieval is well suited to conditions with light cloud contamination. We present here some differential water vapor results from profiles corrupted by both cirrus and polar mesospheric clouds (PMCs).

Recent heightened interest in mesospheric water vapor measurements^{8, 9} has sparked scrutiny of HALOE V19 data because they occasionally exhibit elevated water concentrations near the mesopause, particularly in the polar summer (Fig. 12a) and in the tropics at equinox. It has been suggested that the influence of polar mesospheric clouds (PMCs) could be responsible for some of the observations, and exhaustive sensitivity studies have revealed no other measurement or processing induced error mechanism that could be responsible.¹⁰ To test this hypothesis, we applied the differential water retrieval and compared it to V19 (Fig. 12b and c).

The differential retrieval does indeed produce lower polar mesospheric concentrations, although still relatively high (~9 ppmv). The differences indicate both cirrus (blue regions) and PMC (red area) contamination. Similar results were found in both sunrise and sunset occultations, in both northern and southern hemispheres. However, the differential water retrievals did *not* significantly differ from V19 at

high altitudes in the tropical equinox cases, indicating that these V19 water results may be accurate.

Summary

A novel differential water vapor retrieval technique has been introduced that is insensitive to particulate absorption and requires no *a priori* aerosol information. This improves water retrievals when there is light cloud contamination. Results have been shown for both cirrus and PMC conditions. The differential retrieval is a first step towards extending the HALOE water vapor measurements into the upper troposphere.

4. Forward Model Improvements

Background

The success of reliably sounding the troposphere from space hinges on the ability to correctly model the limb path in the target wavebands. A crucial part of this is an accurate spectral model of all significant absorbing gases. V19 HALOE spectroscopy has been well validated, and produces excellent results in the stratosphere and mesosphere. However, in the increased densities of the troposphere, spectral model errors grow larger and more care must be taken to ensure adequate results.

We have identified three spectral model improvements as most important for tropospheric sounding: more accurate O_3 halfwidths; improved aerosol and cloud

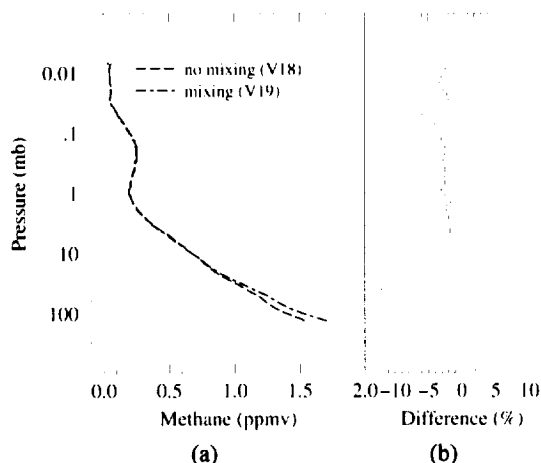


Fig. 13 — HALOE methane for sunrise on 11-Apr-1998 near 57°S, a) Zonal mean (of 15 profiles) with and without CH₄ line mixing. b) Mean difference, differences above 10 mb are primarily from better non-mixed line parameters. Below this, the effect of mixed lines becomes increasingly important.

modeling; and inclusion of CH₄ line mixing. The work to date has focused on the latter, and we describe this here.

Methane line mixing

HALOE uses the gas correlation technique for retrieving HF, HCl, CH₄, and NO. The forward model used here employs a “line-by-line” calculation of the target gases’ spectral cross sections. In this computationally efficient approach, the cross section of each spectral line is found independently. The total cross section is just the sum of all the individual lines. While this is adequate for most molecular transitions and conditions encountered by HALOE, for some CH₄ transitions this approximation begins to fail below the middle stratosphere.

In these conditions, certain lines “mix”—that is, the transitions are quantum mechanically coupled. Each group (usually a pair or triplet of lines) must be considered simultaneously. The spectral cross section of each group is correctly modeled by a matrix formulation, parameterized by a set of “mixing coefficients”.

By simultaneously fitting over 40 high resolution laboratory spectra, Benner et al.¹¹ found 54 groups of CH₄ lines that exhibited significant mixing in the HALOE 3.40 and 3.46 μm channels, used to retrieve HCl and CH₄. Mixing coefficients for these groups were derived. Because the previous line parameters were derived from fits without mixing, some

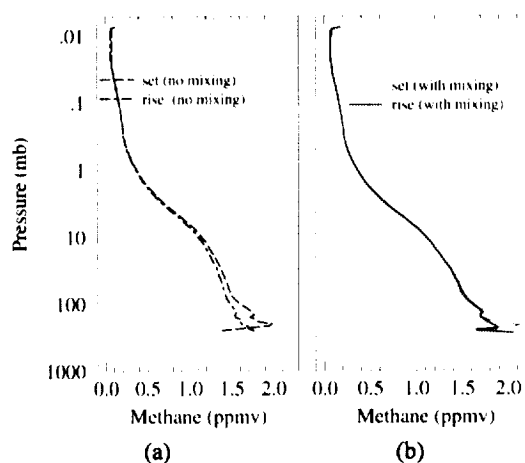


Fig. 14 — HALOE methane sunrise-sunset comparison a) without and b) with CH₄ line mixing. The profiles are averages from 352 coincident rise-set pairs from Jan 1992 to Jan 1998.

non-mixed line parameters were also recomputed.

We incorporated these spectral changes into the appropriate HALOE databases, and modified the HALOE level2 software to include the ability to handle sets of mixed lines. Fig. 13 shows an example of methane retrieved with and without using the line mixing formulation. Differences increase towards the troposphere. High altitude differences are from improved line parameters of unmixed lines. One indication that the line mixing is a beneficial addition to the retrieval process is that sunrise-sunset coincidences now agree much more closely, as demonstrated in Fig. 14.

This initial work was completed in time for inclusion in the delivery of V19 in May 1998. Since then, several advances have been made in understanding the theory of line mixing, and refinements are being made to the spectral fitting code. If tests indicate these changes are significant, they will be included in V20.

5. Fine Vertical Resolution Gas Channel Retrievals

This task has been scheduled for the third fiscal year of the proposal.

6. Improved Temperature-Pressure Retrieval

Work in this area will commence in the coming year.

7. Error Estimates

Work in this area will commence in the coming year.

8. Long Term Trend Analyses

Background

As the data set grows longer it becomes a more valuable research tool, but also more susceptible to the influence of instrument degradation. Trend analyses therefore become more important as the experiment ages. On the other hand, with a more extensive data record, the accuracy of diagnostics increase and better estimates of instrument stability are possible.

Gas-cell content

One of the most crucial parameters to monitor is the gas-cell content. Any change in the concentration of a gas correlation cell (HF, HCl, CH₄ and NO) directly results in a retrieval bias if it is not accurately modeled. For this reason, the conditions of the four cells are closely monitored.

The technique used for detecting gas-cell conditions is a comparison of retrieved mixing ratios at different Doppler velocities (i.e. different beta angles). Any error in modeled gas-cell content will induce a distinct dependence of the retrieved mixing ratios on Doppler shift. This dependence is statistically determined from a large data set, and used to infer the true gas-cell content.

When V18 was developed, it appeared from the limited data set available at the time that there was a trend in the NO gas-cell concentration. V18 therefore employed a linearly decreasing concentration (Fig. 15). However, as the data record grew longer, a trend

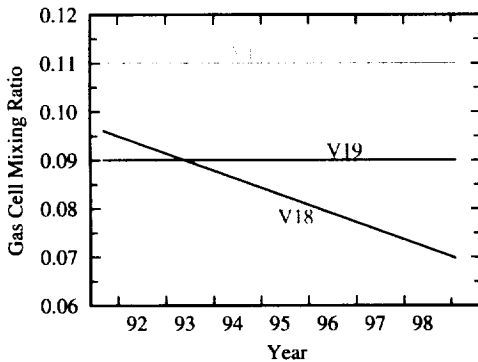


Fig. 15 — HALOE NO gas-cell mixing ratios assumed for Versions 17, 18, and 19. The latest tests indicate that the mixing ratio is stable.

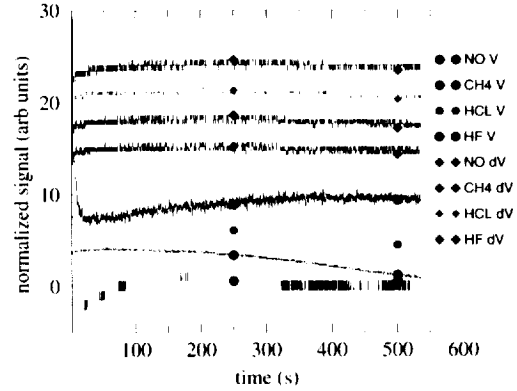


Fig. 16 — Exoatmospheric drift test results for the gas-cell channels, on 8-Feb-1999. In these tests, acquisition of the sun is delayed until it is above the atmosphere. The signals are normalized by their standard deviation. Linear trends are removed during processing so only nonlinear variations are significant. Variations relative to the noise seen here are all within acceptable ranges.

in the retrieved stratospheric NO led us to question the validity of this model. Further Doppler studies on the more extensive data could not support the use of a declining gas-cell concentration, so in V19 a constant concentration was assumed.

Tests on the HF, HCl and CH₄ gas-cells indicate they all remain stable, even within the improved accuracy from the longer data set. This gas-cell analysis will be improved and established as a routine product.

Pointing accuracy

During sunrise occultations, the sun is acquired as low in the as possible and tracked as it traverses the atmosphere. It is possible that the thermal impulse from the initial look at the sun produces a slight motion of the telescope relative to the tracker. Such motion is impossible to measure during a normal sunrise because of the rapidly changing effects of the atmosphere. However, by remaining in stow position until the sun is above the atmosphere and then acquiring and tracking it exoatmospherically, we can directly measure any change resulting from the solar acquisition.

Several such exoatmospheric drift tests have been performed, and Fig. 16 shows results from one recent test. No significant change in detector output has been noticed during these tests, which were performed at a variety of beta angles. The pointing stability appears from these tests to be excellent. Refinements and semiautomatic implementation of these tests are planned.

Summary

Tests on gas-cell content have been carried out. Results for the NO indicate that the concentration of the cell is not changing. This work was completed in time to incorporate in V19. Several on-orbit exoatmospheric drift tests were made to assess the impact of thermal shock during sunrise. The effect appears to be negligible.

9. Data ValidationCorrelative studies

We have begun collecting correlative data sets that can be used for validation of upper tropospheric HALOE measurements. Ozone data will be compared to the battery of *in-situ* data available from the ozonesonde network. V18 data have already been compared in the lower stratosphere and upper troposphere by Bhatt, et al.,⁷ using a set of ozonesonde stations that span the latitude range from 69°S to 74°N. These authors found that cloud screening is essential for use of V18 HALOE measurements in this region. They concluded that when this is done, HALOE and the sondes agree to within ~10% down to 100 mb in the tropics and 200 mb in the extra-tropics. We will use these same ozonesonde stations plus a number of others in order to validate the improved V20 HALOE retrievals, which should extend lower down.

Regarding water vapor, there are a number of correlative data sets available including Lyman- α measurements from the series of aircraft campaigns (e.g. ASHOE, POLARIS), balloon data obtained using the frost-point and Lyman- α hygrometers, recent Raman lidar measurements that extend from the ground to about the tropopause (Sherlock et al., 1998),^{12,13} and aircraft lidar measurements made by the LASE instrument (Browell et al., 1996).¹⁴ A large portion of these data has already been collected and is resident on the HALOE computers. In addition, tropospheric water and ozone data records have been collected in the MOZAIC aircraft campaign, which has been in operation since August 1994. MOZAIC is a project for the autonomous measurement of these gases using instrumentation onboard five AIRBUS A340 aircraft on scheduled flights of commercial airlines (Marenco et al., 1998).¹⁵ We already have these data on hand.

Finally, Dr. Russell is overall co-chair of the international SPARC water vapor assessment study currently under way and this will facilitate collection of the latest and most complete water

vapor data set available worldwide. Finding extensive correlative methane data is more problematical and a search is underway to identify what is available for tropospheric comparisons.

V19 validation

Under this contract, we assist in validating the V19 data product. At this point, all back-days have been validated and V19 has been publicly released. The validation effort involves a number of internal checks on the data, such as sunrise-sunset differences and inter-species comparisons, as well as operational trending and routine limit checks. Careful validation of the V19 product will identify any problems in the current data set that will need to be addressed in V20 algorithm development.

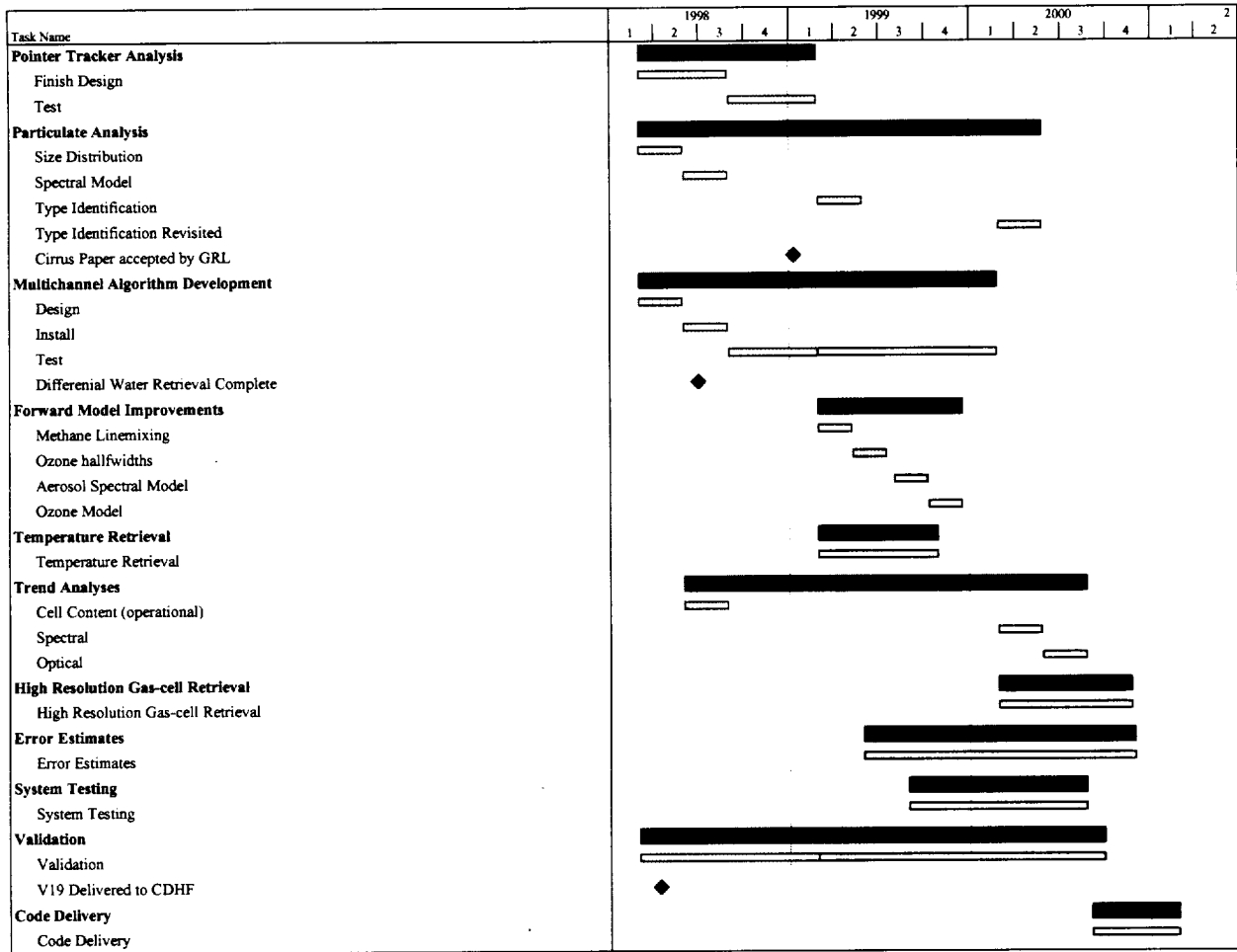
Schedule/Plans

Table 2 shows the schedule of activities. Completed portions of tasks are indicated by green shading of the bars, and red indicates planned work. Milestones are charted as diamonds.

As we enter the second year, we will complete the multichannel retrieval effort, and make additional improvements to the forward models and begin implementing the new temperature retrieval.

With a continued aggressive approach to this complex task over the next two years, V20 will deliver a HALOE dataset significantly improved in both extent and quality.

Table 2 - Project Timelines



Bibliography

- 1 Russell, J. M. III, L. L. Gordley, J. H. Park, S. R. Drayson, W. D. Hesketh, R. J. Cicerone, A. F. Tuck, J. E. Frederick, J. E. Harries and P. J. Crutzen, "The Halogen Occultation Experiment," *J. Geophys. Res.* **98**, 10777-10797, 1993
- 2 Sassen, K., M. K. Griffin and G. C. Dodd, "Optical scattering and microphysical properties of subvisible cirrus clouds, and climatic implications," *J. Appl. Meteorol.*, **28**, 91-98, 1989
- 3 Borrmann, S., S. Solomon, J. E. Dye, B. Luo, "The potential of cirrus clouds for heterogeneous chlorine activation," *Geophys. Res. Letters*, **23**, 2133-2136, 1996
- 4 Kent, G. S., D. M. Winker, M. A. Vaughn, P-H. Wang and K. M. Skeens, "Simulation of Stratospheric Aerosol and Gas Experiment (SAGE) II cloud measurements using airborne lidar data," *J. Geophys. Res.*, **102**, 21795-21807, 1997
- 5 Hervig, M. E. and M. J. McHugh, "Cirrus detection using HALOE measurements," in press, *Geophys. Res. Let.*, March 15 1997.
- 6 Liao, X., W. B. Rossow and D. Rind, "Comparison between SAGE II and ISCCP high-level clouds 1. Global and zonal mean cloud amounts," *J. Geophys. Res.*, **100**, 1121-1135, 1995
- 7 Bhatt, P. P., E. E. Remsberg, L. L. Gordley, J. M. McInerney, V. G. Brackett and J. M. Russell III, "An evaluation of the quality of HALOE ozone profiles in the lower stratosphere," *J. Geophys. Res.*, in press, 1999
- 8 Chandra, S., C. H. Jackman, E. L. Fleming and J. M. Russell III, "The seasonal and long term changes in mesospheric water vapor," *Geophys. Res. Let.*, **24**, 639-642, March 15 1997.
- 9 Nedoluha, G. E., R. M. Bevilacqua, R. M. Gomez, D. E. Siskind, B. C. Hicks, J. M. Russell III and B. J. Connor, "Increases in middle atmosphere water vapor as observed by the Halogen Occultation Experiment and the Ground-based Water Vapor Millimeter-Wave Spectrometer from 1991 to 1997," *J. Geophys. Res.*, **103**, 3531-3544, 1998.
- 10 Russell, J. M. III, L. L. Gordley, G. M. Beaver, E. E. Remsberg, "HALOE water vapor data quality in the mesosphere," presented at *UARS Science Team Meeting*, Pasadena, CA, March 16-18 1998
- 11 Benner, D. C., V. M. Devi, M. A. H. Smith, C. P. Rinsland, G. Guelachvili, L. R. Brown, "Line mixing coefficients in the ν_3 band of $^{12}\text{CH}_4$ and $^{13}\text{CH}_4$," presented at *53rd International Symposium on Molecular Spectroscopy*, Ohio State University, Jun 15-19, 1998
- 12 Sherlock, V. J., A. Garnier, A. Hauchecorne and P. Keckhut, "Implementation and validation of a Raman backscatter lidar measurement of mid and upper tropospheric water vapour," Submitted to *Applied Optics*, 1998
- 13 Sherlock, V. J., J. Lenoble and A. Hauchecorne, "Methodology for the independent calibration of Raman backscatter water vapour lidar systems," Submitted to *Applied Optics*, 1998
- 14 Browell, E. V., S. Ismail, W. M. Hall, A. S. Moore Jr., S. A. Kooi, V. C. Brackett, M. B. Clayton, J. D. W. Barrack, F. J. Schmidlin, N. S. Higdon, S. H. Melfi, D. N. Weightran, "The LASE validation experiment," Proceedings of the 18th International Laser Radar Conference, Berlin, Germany, p289-295, July, 1996.
- 15 Marengo, A., V. Thouret, P. Nedelec, H. Smit, M. Helten, D. Kley, f. Karcher, P. Simon, K. Law, J. Pyle, G. Poschmann, R. Von Wrede, C. Hume, and T. Cook, "Measurement of ozone and water vapor by AIRBUS in-service aircraft: The MOZAIK airborne program, an overview," *J. Geophys. Res.*, **103**, 25631-25642

5/17/99 sent original + dtp to 2592

REPORT DOCUMENTATION PAGE			Form Approved OMB No. 0704-0188	
Public reporting burden for this collection of information is estimated to average 1 hour per response, including the time for reviewing instructions, searching existing data sources, gathering and maintaining the data needed, and completing and reviewing the collection of information. Send comments regarding this burden estimate or any other aspect of this collection of information, including suggestions for reducing this burden, to Washington Headquarters Services, Directorate for Information Operations and Reports, 1215 Jefferson Davis Highway, Suite 1204, Arlington, VA 22202-4302, and to the Office of Management and Budget, Paperwork Reduction Project (0704-0188), Washington, DC 20503.				
1. AGENCY USE ONLY (Leave blank)	2. REPORT DATE March 1999	3. REPORT TYPE AND DATES COVERED Contractor Report		
4. TITLE AND SUBTITLE Yearly Report: HALOE Algorithm Improvements for Upper Tropospheric Sounding			5. FUNDING NUMBERS C NAS5-98076	
6. AUTHOR(S) M. McHugh, L. Gordley				
7. PERFORMING ORGANIZATION NAME(S) AND ADDRESS (ES) GATS, Inc. 11864 Canon Blvd., Suite 101 Newport News, VA 23606			8. PERFORMING ORGANIZATION REPORT NUMBER	
9. SPONSORING / MONITORING AGENCY NAME(S) AND ADDRESS (ES) National Aeronautics and Space Administration Washington, DC 20546-0001			10. SPONSORING / MONITORING AGENCY REPORT NUMBER CR-1999-209234	
11. SUPPLEMENTARY NOTES Technical Monitor: A. Douglass, Code 916				
12a. DISTRIBUTION / AVAILABILITY STATEMENT Unclassified - Unlimited Subject Category: 43 Report available from the NASA Center for AeroSpace Information, Parkway Center/7121 Standard Drive, Hanover, Maryland 21076-1320			12b. DISTRIBUTION CODE	
13. ABSTRACT (Maximum 200 words) This report details the ongoing efforts by GATS, Inc., in conjunction with Hampton University and University of Wyoming, in NASA's Mission to Planet Earth UARS Science Investigator Program entitled "HALOE Algorithm Improvements for Upper Tropospheric Soundings." The goal of this effort is to develop and implement major inversion and processing improvements that will extend HALOE measurements further into the troposphere. In particular, O ₃ , H ₂ O, and CH ₄ retrievals may be extended into the middle troposphere, and NO, HC1 and possibly HF into the upper troposphere. Key areas of research being carried out to accomplish this include: pointing/tracking analysis; cloud identification and modeling; simultaneous multichannel retrieval capability; forward model improvements; high vertical-resolution gas filter channel retrievals; a refined temperature retrieval; robust error analyses; long-term trend reliability studies; and data validation. The current (first-year) effort concentrates on the pointer/tracker correction algorithms, cloud filtering and validation, and multi-channel retrieval development. However, these areas are all highly coupled, so progress in one area benefits from and sometimes depends on work in others.				
14. SUBJECT TERMS HALOE, UARS, remote sensing			15. NUMBER OF PAGES 18	
			16. PRICE CODE	
17. SECURITY CLASSIFICATION OF REPORT Unclassified	18. SECURITY CLASSIFICATION OF THIS PAGE Unclassified	19. SECURITY CLASSIFICATION OF ABSTRACT Unclassified	20. LIMITATION OF ABSTRACT UL	